III. SOLID-STATE MICROWAVE ELECTRONICS*

Academic and Research Staff

Prof. P. L. Penfield, Jr.
Prof. D. H. Steinbrecher
Dr. K. F. Kunzi

Graduate Students

A. Chu
R. W. Freund
G. P. Hom
V. T. Kjartansson
G. K. Montress
M. S. Navarro
Y. K. Yee

A. NOISE-FIGURE MEASUREMENTS ON BARITT DIODE NEGATIVE-RESISTANCE AMPLIFIERS AT 4 GHz

The most common semiconductor diodes exhibiting transit-time negative resistance at microwave frequencies are those relying on avalanche breakdown at a reverse-biased p-n junction for carrier injection into a drift space. Recently, however, there has been considerable interest in the so-called BARITT (Barrier Injection Transit Time) diodes, which differ from avalanche diodes, in that minority carriers are injected into the drift region at a forward-bias contact.[1] Such devices have been used to generate up to 50 mW cw at C-band with an efficiency ~1.8%.[2] The absence of avalanche breakdown in BARITT operation makes it an inherently low-noise device and amplifier noise figures as low as 15 dB at ~6.68 GHz have been measured thus far.[3] Small-signal analysis[4] indicates that noise measures as low as 3 dB may be achieved with BARITT diodes.

We have fabricated[5] metal n-type silicon p^+-type silicon diodes and measured negative resistance and amplifier noise characteristics. Fifteen different amplifiers have been built and tested. Typical results are as follows:

Noise figure	12 dB
Voltage gain-bandwidth product	170 MHz
Center frequency	4.1 GHz
Maximum stable gain	~50 dB
Bias current	3.5 mA
Bias voltage	25 V

The minimum noise figure measured was 11 dB ± .5 dB.

Circuit losses were evaluated by de-imbedding procedures and we found that the diode series resistance and other circuit losses account for approximately 1-1.5 dB of

*This work was supported principally by the Joint Services Electronics Programs (U.S. Army, U.S. Navy, and U.S. Air Force) under Contract DAAB07-71-C-0300 and in part by California Institute of Technology Contract 952568.

the total measured noise figure. Then the contribution to the amplifier noise figure by the diode junction is typically 10.5 dB. This compares favorably with values predicted by Statz, Pucel, and Haus.[4] Their theoretical predictions indicate that the minimum noise figure would occur near the maximum frequency at which the diode exhibits negative resistance. For the diodes that we tested, this maximum frequency was approximately 6 GHz, while the amplifier operating frequency was typically 4 GHz. We might therefore expect that even lower noise figures could be obtained at frequencies higher than those at which our measurements were made.

A paper entitled "Noise-Figure Measurements on BARITT Diode Negative Resistance Amplifiers at 4 GHz" by D. H. Steinbrecher and M. G. Adlerstein will be presented at the Device Research Conference, Edmonton, Alberta, Canada, on June 21-24, 1972, describing this work in more detail.

D. H. Steinbrecher

References

1. H. W. Ruegg, "A Proposed Punch-Through Microwave Negative-Resistance Diode," IEEE Trans., Vol. ED-15, p. 577, August 1968.
2. D. J. Coleman and S. M. Sze, "A Low-Noise Metal-Semiconductor (MSM) Microwave Oscillator," Bell System Tech. J. 50, 1695-1699 (1971).
3. S. G. Liu and J. J. Risko, "Low-Noise Punch-Through P-N-ν-P, P-N-P, and P-N-Metal Microwave Diodes," RCA Rev. 32, 636-644 (1971).
4. H. Statz, R. A. Pucel, and H. A. Haus, "Velocity Fluctuations in Metal-Semiconductor-Metal Diodes," Raytheon Technical Memorandum T-904 (to be published).
5. Devices were fabricated at Raytheon Research Laboratories, Waltham, Mass., under the supervision of Dr. M. G. Adlerstein.

B. BARITT DIODES

Barrier Injection Transit Time (BARITT) diodes have been fabricated for use as low-noise microwave amplifiers. These devices utilize a forward-biased Schottky barrier formed from an anneal of aluminum and silicon, together with a reverse-biased p-n junction. Direct-current characteristics of the diodes have been tested. Reach-through voltages in the range 15-25 V have been measured. Capacitance measurements and device mounting in a microwave package must be done before microwave measurements may be taken. It is expected that this will soon be accomplished.

G. K. Montress, M. G. Walker

C. MIXER DEVELOPMENT AT 100 GHz FOR ATMOSPHERIC OZONE RESEARCH

We are developing a low-noise mixer at frequencies near 100 GHz for atmospheric research and, possibly, for radio astronomy. The mixer will first be used to study the

stratospheric O_3 emission line at 101.737 GHz and, we hope, the diurnal variation in mesospheric O_3.

Previous measurements by J. Rutzki[1] have put an upper limit of $5 \cdot 10^{10}$ cm^{-3} at 50 km and 10^9 cm^{-3} at 80 km on the number density of mesospheric O_3. A first single-ended mixer has been constructed by use of a tapered waveguide section for matching the diode and a fixed quarter-wavelength short. Lincoln Laboratory supplied the Schottky-barrier diodes used in this mount. The results of a first test of some diodes are summarized in Table III-1. Diode No. 6 has been used in a radiometer at 100 GHz. The double-sideband noise temperature is approximately 3000°K using an IF amplifier with ~2.5 dB noise figure and a bandwidth of 40 MHz-80 MHz. For all noise measurements we used a 10,000°K noise tube and a precision attenuator. It is hoped that with better diodes and preamplifiers we will decrease the noise temperature ~30%.

Table III-1. Performance of different diodes at 55 and 100 GHz. All data except for the 100-GHz measurements have been supplied by Lincoln Laboratory, M.I.T.

Diode No.	R_c (Ω)	C_r (ff) Zero Bias	Diode (μm) Dot Diameter	NF (dB)	
				55 GHz	100 GHz
5	10.8	9.0	1.5	5.51	7.5
6	11.3	8.1	1.0	5.48	8.0
7	10.4	9.5	1.5	5.27	8.5
8	10.3	8.9	1.0	5.54	7.5
10	14.8	8.0	1.5	7.98	8.5

I wish to thank B. Clifton, of Lincoln Laboratory, M.I.T., for supplying the diodes and D. C. Papa of the Radio Astronomy Group of the Research Laboratory of Electronics for designing the mount. I also wish to acknowledge helpful discussions with D. Chick, of Lincoln Laboratory, M.I.T., and with Professor D. Steinbrecher.

K. F. Kunzi

References

1. J. E. Rudzki, "Remote Sensing of Mesospheric Ozone," Ph.D. Thesis, Department of Electrical Engineering, M.I.T., January 1971.

D. LOW-NOISE INTERMEDIATE-FREQUENCY AMPLIFIERS FOR 55-GHz RADIOMETERS

Our work on low-noise intermediate-frequency amplifiers was described in general in a previous report.[1]

We have now completed s-parameter measurements on the Type AT-17A transistor in the frequency range 45-900 MHz. We are only interested in passband frequencies up to ~500 MHz, but stability considerations for the broadband case require measurements well above that.

The special circuit analysis program MARTHA has been used to model the transistor numerically in terms of its s-parameters directly. Excellent agreement has been obtained between computer analysis of amplifier circuits built thus far and actual measurements.

Prospective modifications to improve the passband flatness have been explored with the computer simulation. Some of these, notably a cascade configuration, should be tried in practice, and the effect on the noise figure studied.

Four dual amplifiers of the 10-110 MHz variety (described in the previous report) have been built by the Radio Astronomy Group, and one of them is shown in Fig. III-1.

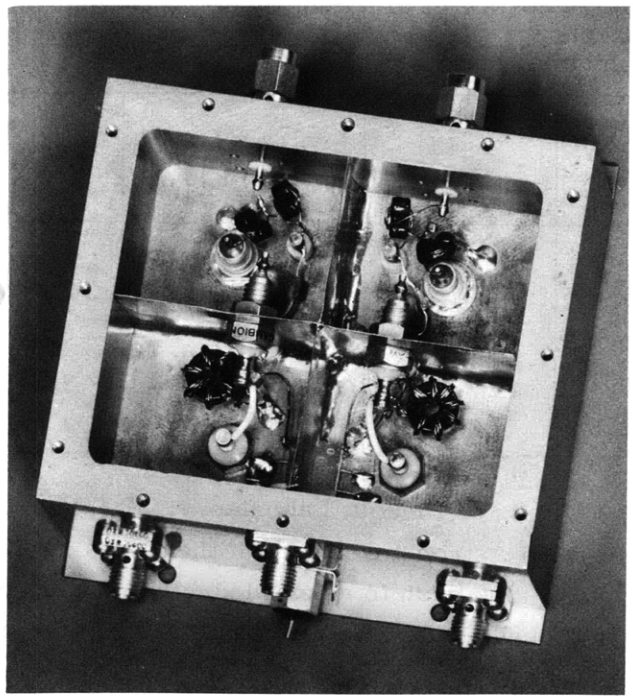

Fig. III-1. Low-noise 10-110 MHz dual preamplifier.

It contains two amplifiers, one for each arm of a balanced mixer, with their outputs combined in a hybrid.

V. T. Kjartansson

References

1. Quarterly Progress Report No. 105, Research Laboratory of Electronics, M.I.T., April 15, 1972, pp. 13-15.

E. PEAK-LOCKING APPROACH FOR STABILIZATION OF HIGH-RESOLUTION MASS SPECTROMETER*

1. Introduction

A peak-locking approach for the stabilization of a CEC-21-110 high-resolution mass spectrometer has been proposed.[1] The hardware implementation of this project is now under way. One of the constraints during this phase of the work is to introduce modifications and perform tests with a minimum of interruption of the regular operation of the instrument. For these purposes, the control unit is being built as an independent unit that can be connected to the magnet by means of a single switch.

This report describes the addition of a set of deflection plates to the three-way slit of the mass spectrometer, the construction of a low-temperature-coefficient sensing resistor, and the control circuitry.

2. Modification of the Exit Slit

Figure III-2 shows the set of deflection plates mounted on the three-way exit slit. The plates do not protrude beyond the plane of the screws at the left. The clearance between the screws and the pole face is approximately 15 mils. The ion beam lies in

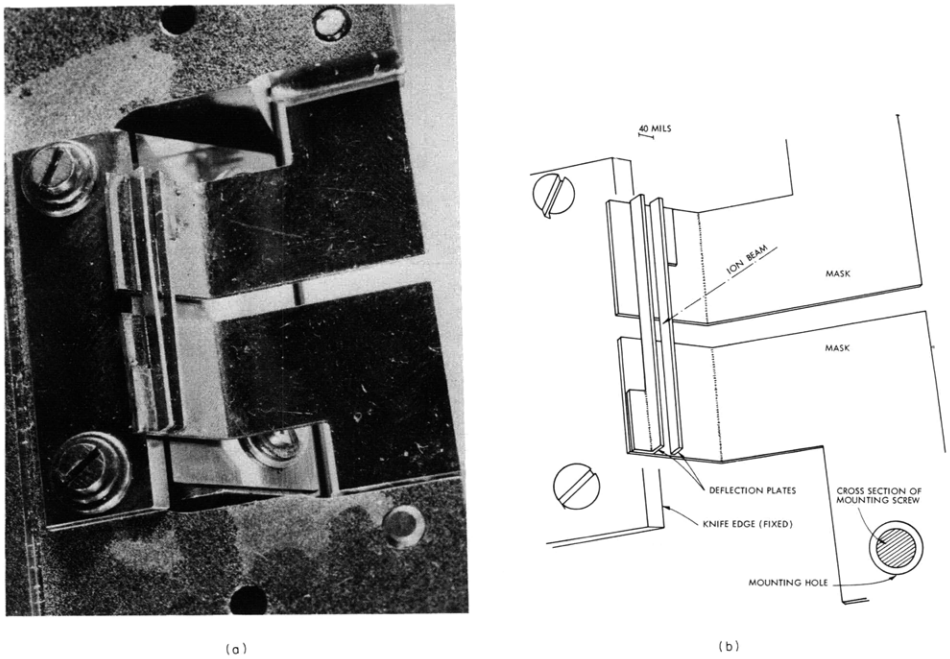

Fig. III-2. Deflection plates assembly. (a) Photograph. (b) Diagram.

*This work was supported by the National Institutes of Health (Grant RR00317) from the Biotechnology Resources Branch, Division of Research Resources.

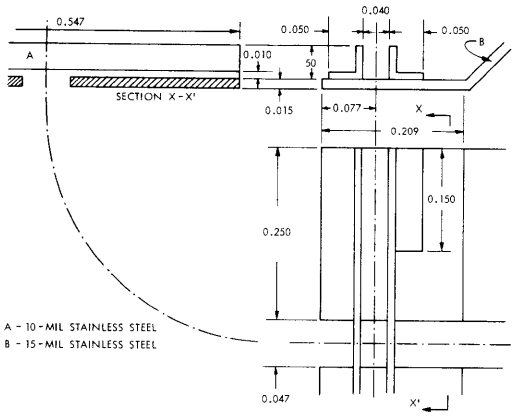

(a)

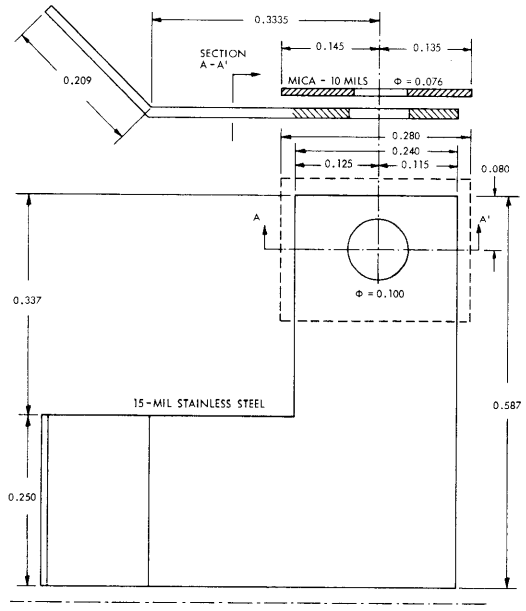

(b)

Fig. III-3. (a) Deflection plates.
(b) Mask.

the plane of symmetry of the deflection plates; the height of the beam is trimmed by the mask, which serves as support and electrical connections for the plates. The mask is electrically isolated from the slit by means of inorganic mica washers. The diameter of the mounting holes is such that when the plates are aligned symmetrically with respect to the fixed knife edge, and 40 mils apart from each other, the mask is isolated from the mounting screws. Figure III-3 shows the dimensions of the deflection plates and the modified mask.

Machining of the assembly to a tolerance of .5 mils involved manufacturing special jigs. Figure III-4a shows the jig that was used for bending the masks, and Fig. III-4b the jig for spot-welding the deflection plates to the masks. Four

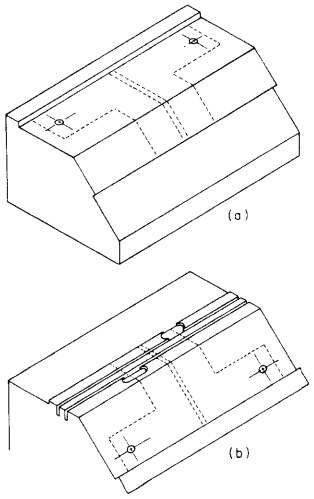

Fig. III-4.

(a) Jig for bending the masks.
(b) Jig for spot-welding the deflection plates.

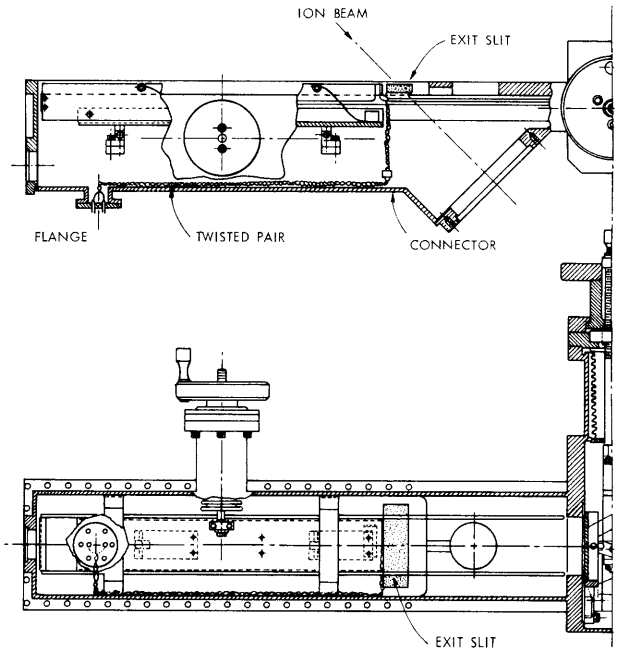

Fig. III-5.

Connections to the deflection plates.

sets of plate assemblies were built. The best set was selected by direct trial on the slit and examination under an optical comparator. A flange with a pair of heliarc-welded standoffs was built to bring the connections from the deflection plates, as illustrated in Fig. III-5. The twisted pair of wires was laid along the corners of the photoplate box; the operation of the photoplate assembly was not perturbed. The modified exit slit was installed and no leakage or degassing occurred.

3. Sensing Resistor

The feedback control circuit compares the voltage developed across the sensing resistor by the magnet's current and the reference voltage. Consequently, the stability of this resistor is of great importance. Three alternatives were considered: a standard resistor, a Manganin wire resistor, and a bank of bulk metal film resistors (Vishay Model S-102). Table III-2 summarizes the temperature coefficients.

Table III-2. Summary of temperature coefficients.

Resistor	Temperature Coefficient (ppm)	Temperature Range (°C)	Zero Temperature Coefficient (°C)
Standard	15	15-35	
Standard Manganin	15	15-35	22
Shunt Manganin	15	40-60	50
Bulk Metal Film	.9	25-60	25

Because of cost, we did not use an oven; instead we chose the bulk metal film resistor bank. Several samples of Vishay S-102 resistors were tested with a Wheatstone's bridge and cycled in an oven. The manufacturer's specifications were confirmed. A .283 Ω sensing resistor was built by connecting thirty-six 10.2 Ω ±.1% resistors in parallel. The maximum current through the magnet's coil is 5 A; therefore, the power dissipation is 7.09 W. The dissipation per unit is 197 mW, and the rating is 300 mW.

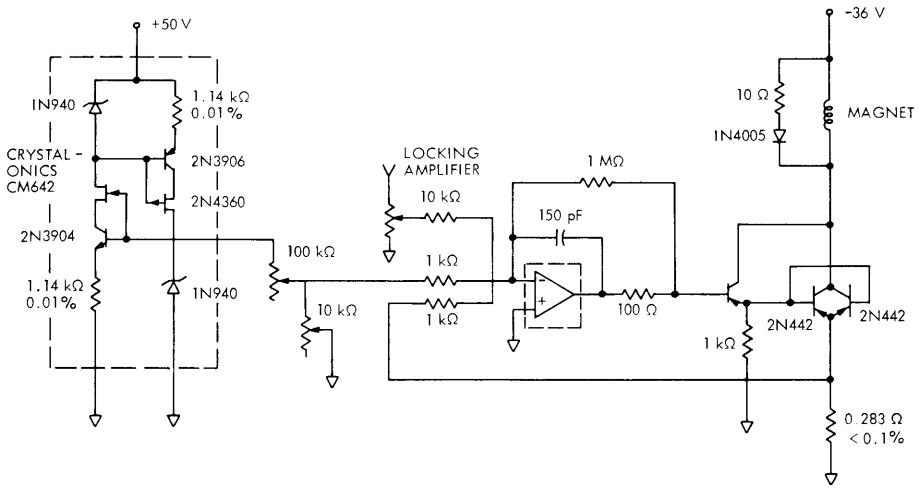

Fig. III-6. Control circuit.

The resistor bank is heat sunk. The temperature rise was evaluated as 3° C above ambient; experimental results are not yet available.

4. Control Circuit

The control circuit is illustrated in Fig. III-6. The operational amplifier is Philbrick Nexus 1700-02 with a typical offset voltage of ±0.02 μV/deg C and a guaranteed voltage drift of ±0.2 μV/deg C. The large-signal frequency response is 1 MHz at unity gain. This operational amplifier did not meet the 6 dB per octave roll-off specification of the manufacturer, and, therefore, frequency compensation and a minor feedback loop around the operational amplifier were required. The effect of the decreased open-loop gain is degradation of the magnet current stability to 15-20 ppm.

A. Chu

References

1. A. Chu, "Peak-Locking Approach for Stabilization of High-Resolution Mass Spectrometers," Quarterly Progress Report No. 104, Research Laboratory of Electronics, M.I.T., January 15, 1972, pp. 89-95.
2. L. L. Evans, "Biasing FET's for Zero D-C Drift," Electro-Technology, Vol. 74, pp. 93-96, August 1964.

F. MODULATOR IMBEDDING NETWORKS FOR P-I-N DIODES

This report describes a matching technique for a P-I-N diode and a 50 Ω line in order to obtain the proper reflection phase relationships for a 0-180° phase modulator.

1. Problem

The optimum operating condition for this modulator is achieved when the two impedance points, "on" and "off", produce equal-magnitude but opposite-phase reflection coefficients. The problem (Fig. III-7) involves simultaneous transformation of two given impedances by means of a single coupling network.

In hyperbolic non-Euclidean geometry[1] any circle orthogonal with the limb of the Smith chart is defined as a hyperbolic straight line. By drawing a hyperbolic straight line through the points z_1 and z_2 (on and off impedances), the problem is reduced to a single-valued impedance matching by locating the middle point of the segment z_1 and z_2 and matching this value to the 50 Ω line. Since under lossless transformations distances are preserved, the values of z_1 and z_2 will produce equal-magnitude but opposite-phase reflection coefficients.

The non-Euclidean middle point between two points $r_1 + jx$ and $r_2 + jx$ on a constant reactance curve of the Smith chart is given[1] by

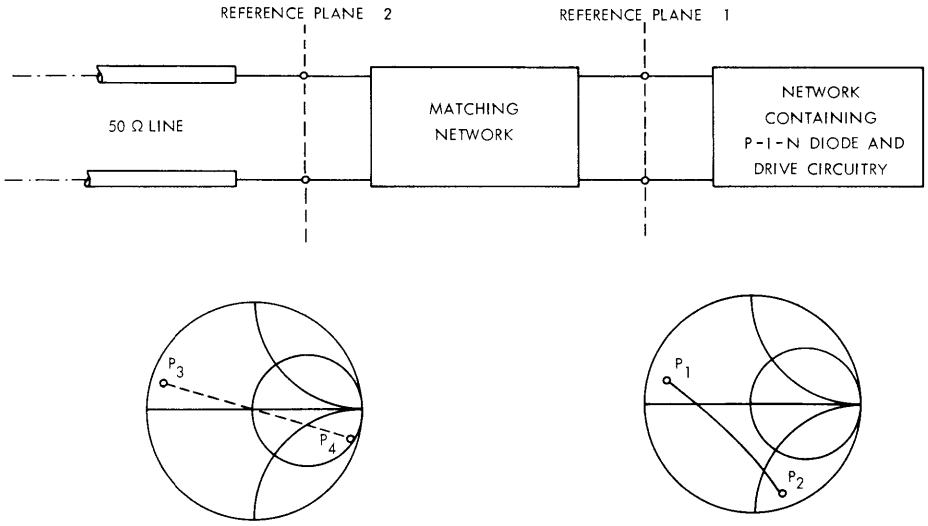

Fig. III-7. P-I-N diode matching network impedance as a function of bias, normalized to 50 Ω.
Lower right: Measured at reference plane 1. With diode "on", $P_1 = r_1 + jx_1$; with diode "off", $P_2 = r_2 + jx_2$.
Lower left: Measured at reference plane 2. The reflection coefficient at P_3 should equal in magnitude the reflection coefficient at P_4.

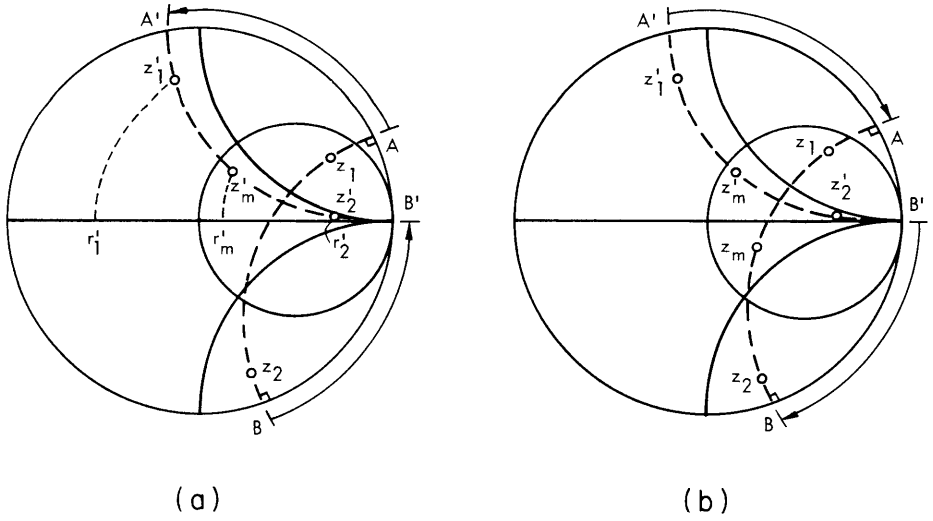

Fig. III-8. (a) Location of the middle point, m, by means of Eq. 1.
(b) Location of the middle point, z_m, at the original reference plane.

$$r_m = \sqrt{r_1 \cdot r_2}. \tag{1}$$

Since our hyperbolic straight line is located at an arbitrary position, we rotate this line until it lies on a constant reactance curve and then locate the middle point by means of (1), as indicated in Fig. III-8. Once the middle point is determined, it is transformed back to the original reference plane. Schematically, the steps for determining z_m at the original reference plane are indicated in Fig. III-9.

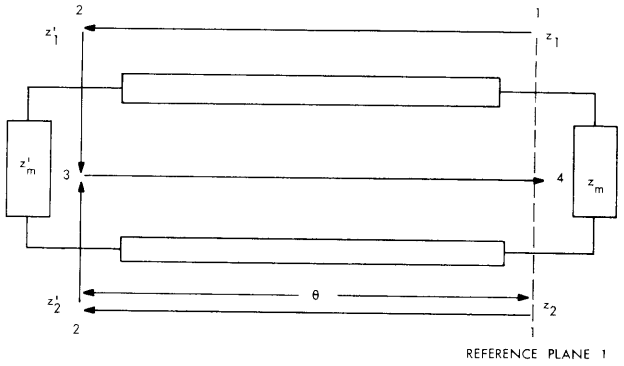

Fig. III-9. Determination of z_m at the original reference plane.

The problem can be solved analytically using the ABCD parameters of a 1 Ω lossless transmission line,

$$z'_a = \frac{z_a \cos\theta + j \sin\theta}{j z_a \sin\theta + \cos\theta} \qquad a = 1, 2, \tag{2}$$

and, solving for

$$I_m[z'_1] = I_m[z'_2], \tag{3}$$

we get

$$\tan\theta = \frac{-b \pm \sqrt{b^2 - 4ac}}{2a}, \tag{4}$$

where

$$b = |z_2|^2 - |z_1|^2$$

$$a = |z_1|^2 \cdot X_2 - |z_2|^2 \cdot X_1$$

$$c = X_1 - X_2.$$

Taking the value of tan θ, we calculate r'_1 and r'_2 by means of (2). The real part of the middle point is given by (1), the imaginary part is given by (3). Having the real and imaginary parts of z'_m, we move in the opposite direction to the original reference plane to get z_m, the non-Euclidean middle point of the segment z_1-z_2.

2. Matching Network

A general solution of the matching problem involving two transmission lines, λ/4 and λ/8, has been previously described.[2] In some cases, the following matching technique may be more desirable.

When the impedance z_m is located inside the circle R = 1 or inside the circle $R^2 + X^2 = R$, the matching network will be a single transmission line. The non-Euclidean

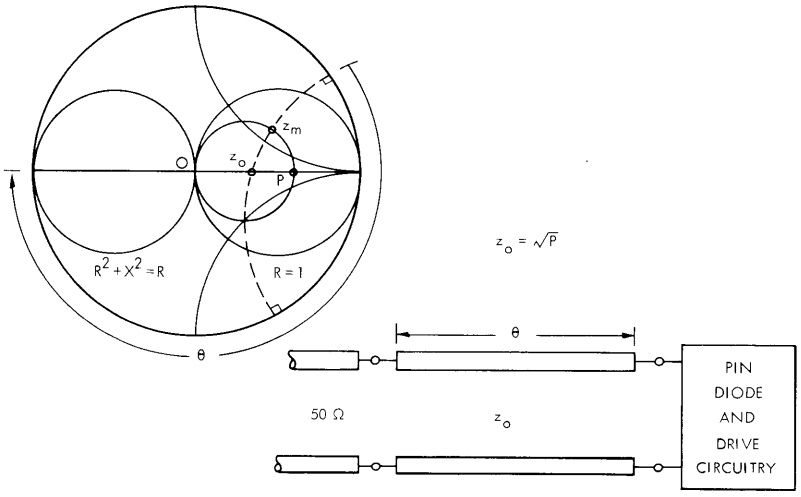

Fig. III-10. Determination of length and characteristic impedance of the matching network.

center of the circle through z_m will be the characteristic impedance, and the length is given by the intercept of the hyperbolic straight line through z_m and z_o with the Smith chart, as illustrated in Fig. III-10.

3. Broadbanding Techniques

Having the values of z_m, in a given frequency band, it is possible to find a model of the diode by means of the locus of z_m on the Smith chart. Once we know the model of the diode, the broadband match is achieved by using Fano's method.[3]

M. S. Navarro

References

1. R. L. Kyhl, "The Use of Non-Euclidean Geometry in Measurements of Periodically Loaded Transmission Lines," IRE Trans., Vol. MTT-4, No. 2, p. 111, April 1956.

2. D. H. Steinbrecher, "An Interesting Impedance Matching Network," IEEE Trans., Vol. MTT-15, No. 6, p. 382, June 1967.

3. R. M. Fano, "Theoretical Limitations on the Broadband Matching of Arbitrary Impedances," J. Franklin Inst. 249, 57-154 (1950).